3. Mechanisms of Laminar Mixing.

Identification and understanding of the phenomena related to the process of mixing on the molecular scale is necessary when a general model of micromixing is to be formulated. In this chapter elementary mechanisms governing micromixing in very viscous fluids of **Sc>>1** (liquids) are presented and discussed. The considerations are restricted to isothermal mixing of Newtonian, incompressible and fully miscible liquids; the effects of liquids incompatibility are also briefly presented.

As the mixing of very viscous liquids is concerned with low Reynolds numbers only the laminar flow is considered. It is also assumed that the liquids viscosity and density as well as diffusion coefficients of reactants and chemical kinetics rate constants are not affected by concentration of reactants.

3.1. Molecular Diffusion in Deformed Liquid Elements.

The literature indicates that mixing in very viscous, completely miscible liquids proceeds by deformation and distribution of liquid elements in the mixed volume. This process is schematically shown in figure 3.1. However, the convective mixing which decreases segregation scales and increases the contact surface area between mixed liquids cannot decrease the concentration variance based on the distribution of local concentration in the system. Mixing on the molecular scale which directly influences chemical reactions is equivalent to molecular diffusion.

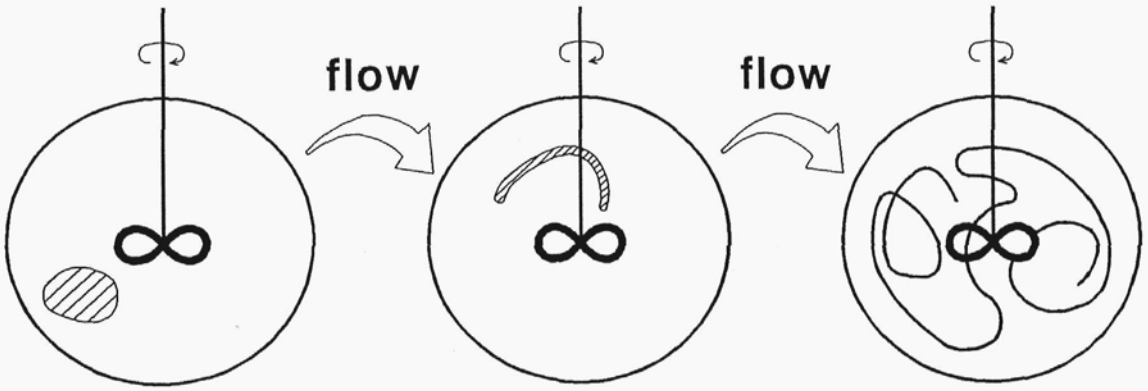

Figure 3.1. Deformation and distribution of the minor component in a mixer.

However, mixing of liquids by molecular diffusion requires long times; notice that for the scale of segregation s_0=1 **m** and diffusion coefficient $D=10^{-10}$ **m**^{2}/**s** the characteristic time

constant equals

$$t_D = s_0^2/D = 10^{10}[s] = 317.1[years] . \quad (3.1)$$

Mechanical mixing reduces scales of segregation and accelerates mixing on the molecular level; decreasing of the scale $\mathbf{s_0}$ to $\mathbf{s_0'=10^{-3}\ m}$ results in

$$t_D^{/} = (s_0^{/})^2/D = 10^4[s] = 2.78[hours] \quad (3.2)$$

and in the case of $\mathbf{s_0''=10^{-4}\ m}$ one has only

$$t_D^{//} = (s_0^{//})^2/D = 10^2[s] = 1.67[\text{min}] . \quad (3.3)$$

The mechanism of acceleration of mixing is however more complex than only decreasing of scale of segregation and increasing exchange area but includes increasing of the concentration gradients which are in turn softened by molecular diffusion.

To illustrate this let us consider a process of diffusion of an inert tracer from a stretched lamina to infinite environment. The lamina of initial thickness $\mathbf{s_0}$ (shown in figure 3.2) is stretched by two dimensional stagnant flow. In this case, flow is characterized completely by the rate of stretch - α [21]:

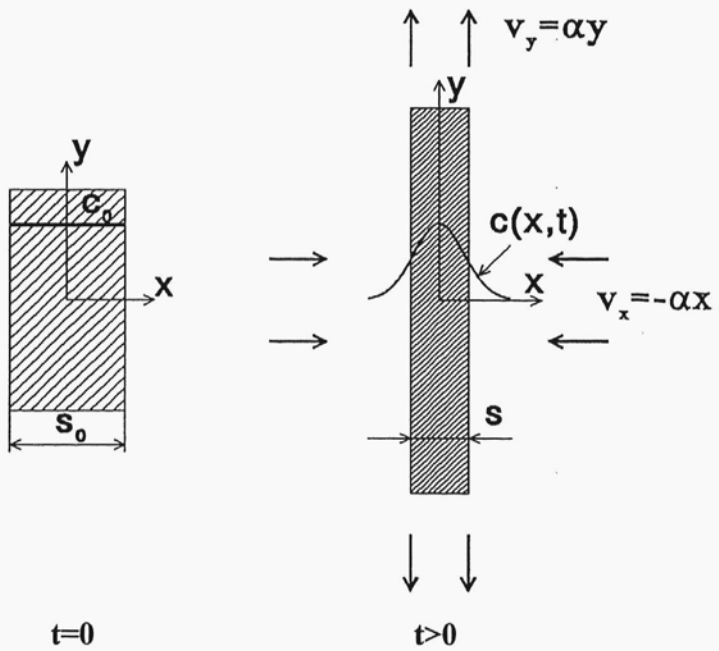

Figure 3.2. Diffusion outward a stretched lamina.

$$v_x = -\alpha \cdot x , \quad v_y = \alpha \cdot y , \quad v_z = 0 . \quad (2.12)$$

The lamina is elongated, so its thickness decreases

$$\frac{1}{s} \cdot \frac{ds}{dt} = -\alpha \quad (3.4)$$

and for α=**const**:

$$s = s_0 \cdot \exp(-\alpha \cdot t) . \quad (3.5)$$

It is also assumed that there is no variation of the slab structure in directions **y** and **z** so the problem is one dimensional. The differential tracer balance, the boundary and the initial conditions are thus as follows:

$$\frac{\partial c}{\partial t} + v_x \cdot \frac{\partial c}{\partial x} = D \cdot \frac{\partial^2 c}{\partial x^2} , \qquad \textbf{(3.6a)}$$

$$c(x \to \pm\infty, t) = 0 , \qquad \textbf{(3.6b)}$$

$$c(x,0) = \begin{cases} 0 & x \le -s_0/2 \\ 1 & -s_0/2 < x < s_0/2 \\ 0 & s_0/2 \le x \end{cases} . \qquad \textbf{(3.6c)}$$

To get rid of convective term in equation (3.6a) one can use the dimensionless variables:

$$\xi = \frac{x}{s} , \qquad \textbf{(3.7a)} \qquad \tau = \int_0^t \frac{D\,dt'}{s^2(t')} , \qquad \textbf{(3.7b)} \qquad C = \frac{c}{c_0} . \qquad \textbf{(3.7c)}$$

Notice that the "warped time" - τ [21] reflects the total effect of deformation, so when expressed by variables ξ and τ the material balance simplifies to

$$\frac{\partial C}{\partial \tau} = \frac{\partial^2 C}{\partial \xi^2} \qquad \textbf{(3.8a)}$$

with the boundary and initial conditions:

$$C(\xi \to \pm\infty, \tau) = 0 , \qquad \textbf{(3.8b)}$$

$$C(\xi,0) = \begin{cases} 0 & \xi \le -1/2 \\ 1 & -1/2 < \xi < 1/2 \\ 0 & 1/2 \le \xi \end{cases} . \qquad \textbf{(3.8c)}$$

Following Carslaw and Jaeger [65, p.53], the analytical solution of equations (3.8) reads:

$$C(\xi,\tau) = \frac{1}{2 \cdot \sqrt{\pi \cdot \tau}} \cdot \int_{-1/2}^{1/2} \exp\left[-\frac{(\xi - \eta)^2}{4 \cdot \tau} \right] d\eta . \qquad \textbf{(3.9)}$$

Let the mixing time be defined as the time required to half the tracer concentration at the symmetry surface of the lamina. The related "warped time" is equal to:

$$\tau_{1/2} \cong 0.275 . \qquad \textbf{(3.10)}$$

The mixing time can be recalculated from $\tau_{1/2}$ with the use of equations (3.5) and (3.7b):

$$t_{E1/2} = \frac{1}{2 \cdot \alpha} \cdot \ln\left(2 \cdot \tau_{1/2} \cdot \frac{\alpha \cdot s_0^{\,2}}{D} + 1 \right) \cong \frac{1}{2 \cdot \alpha} \ln\left(0.55 \cdot \frac{\alpha \cdot s_0^{\,2}}{D} + 1 \right) . \qquad \textbf{(3.11)}$$

When there is no deformation in the system the mixing time reaches its upper bound:

$$t_{D1/2} = \tau_{1/2} \cdot s_0^2 / D \cong 0.275 \cdot s_0^2 / D \ . \qquad (3.12)$$

Figure 3.3 shows how increasing of the stretch rate α, equivalent to decreasing the characteristic time scale of deformation

$$t_F = 1/\alpha \ , \qquad (3.13)$$

decreases the time of mixing $t_{E1/2}$. This example indicates how significant is the effect of deformation and shows that all the models neglecting deformation must lead to superficial results.

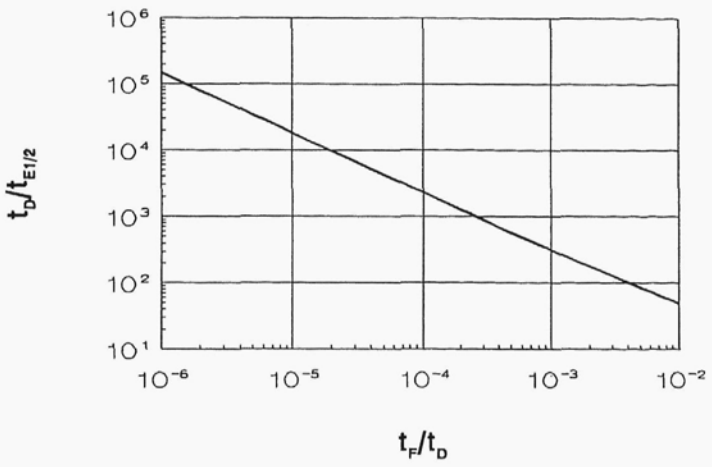

Figure 3.3. Acceleration of molecular diffusion by elongation.

However, one should remember that the deformation of liquid elements can also retard molecular mass transfer. Let us consider again, the system shown in figure 3.2 but for negative values of the stretch rate - α. In this case the thickness of the lamina increases, which decreases the intermaterial area per unit volume and flattens the concentration gradients. This phenomenon has very serious consequences - the orientation of the intermaterial surface with the respect to the principal axes of stretching must also affect the rate of mixing.

Let us consider this problem in more detail, starting from a simple example of a linear shear flow sketched in figure 3.4a.

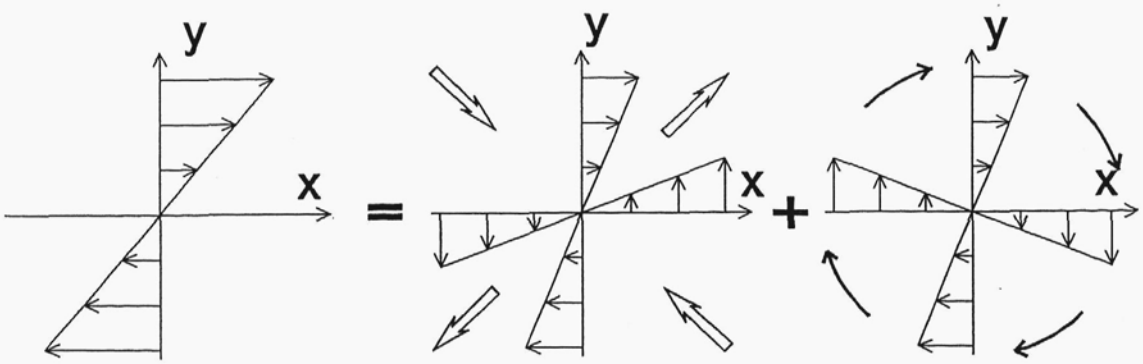

shear flow **deformation** **rotation**

Figure 3.4a. **Figure 3.4b.** **Figure 3.4c.**

Decomposition of a two-dimensional shear flow.

As discussed by Ranz [21] in the close proximity of the material point, the flow can be decomposed into pure deformation and rigid body rotation. Figure 3.4 shows this decomposition; a simple shear flow (a) is decomposed into deformation (b) consisting of uniform extension and contraction, and "rigid body rotation" (c), which does not influence directly mixing. This operation can be generalized as decomposition of the velocity gradient tensor into two parts: symmetric (deformation) and antysymmetric (rotation):

$$Grad\vec{v} = \frac{1}{2}\cdot\left[(Grad\vec{v}) + (Grad\vec{v})^T\right] + \frac{1}{2}\cdot\left[(Grad\vec{v}) - (Grad\vec{v})^T\right] = \overline{\overline{D}} + \overline{\overline{\Omega}} \ . \qquad (3.14)$$

Let us start from the situation, when the velocity gradient tensor has only symmetric part. In this case the intermaterial surface tends to orient itself along the principal axes of strain. In the case of two-dimensional, elongation (figure 3.5) the lamina initially deflected by angle ψ_0 from the main axis of stretching (extension) will change its orientation decreasing finally ψ to zero.

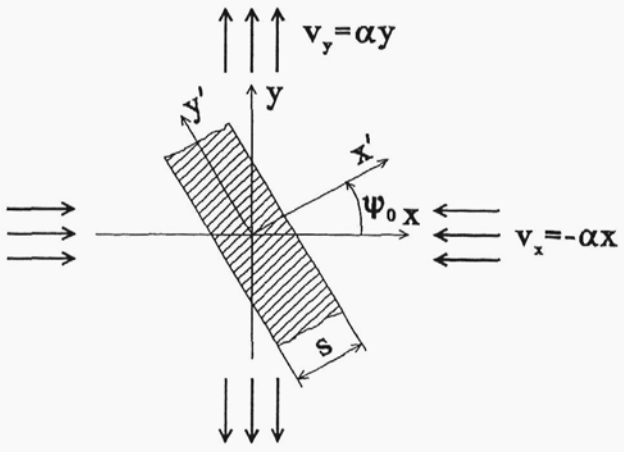

Figure 3.5. Lamina stretched and rotated by a two-dimensional elongation flow.

In the coordinate system moving with the lamina **(x′, y′)**, the stretching flow is characterized by the stretch rate [21]:

$$\alpha' = -\frac{1}{s}\cdot\frac{ds}{dt} = (\cos^2\psi - \sin^2\psi)\cdot\alpha \ . \qquad (3.15)$$

The ratio α'/α plotted against ψ_0 in the figure 3.6 indicates that the fastest elongation and consequently the fastest generation of the intermaterial area per unit volume takes place at ψ=**0°** or ψ=**180°** (with $\alpha'=\alpha$). On the other hand, for ψ=**90°** or ψ=**270°** one has the fastest rate of lamina thickening (with $\alpha'=-\alpha$). Diagonal orientation with the respect to the principal axes of deformation results neither in thinning nor thickening (α'=**0**).

Generally, the rate of changing orientation by the lamina is given by:

$$\frac{d\psi}{dt} = -\alpha\cdot\sin(2\cdot\psi) \ . \qquad (3.16)$$

This relation shows how the lamina tends to orient itself along the direction of the fastest elongation; compare figures 3.6 and 3.7.

The above conclusion may not be true when the antysymmetric part of the velocity gradient tensor does not vanish in the close proximity of the considered material point. The orientation

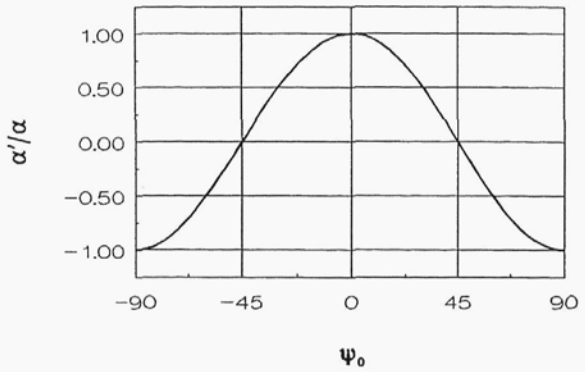

Figure 3.6. The effect of ψ_0 on stretching rate of the lamina.

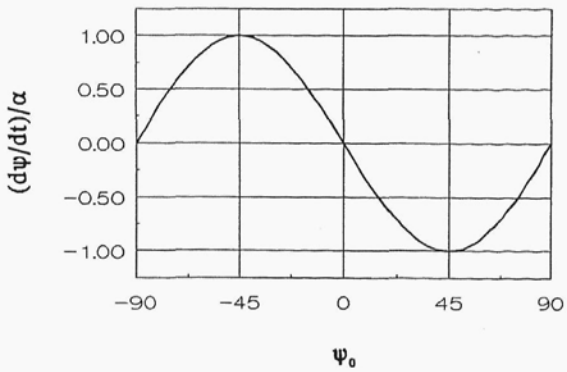

Figure 3.7. The effect of ψ_0 on rotation rate of the lamina.

of the intermaterial surface becomes less dependent on the rate of strain tensor due to influence of rotation. It is even possible that in the close proximity of the material point, the intermaterial surface rotates, being periodically stretched and contracted. To illustrate influence of the non-vanishing rotation tensor - $\overline{\overline{\Omega}}$ on the rate of mixing, let us consider the system with a simple shear shown in figure 3.8.

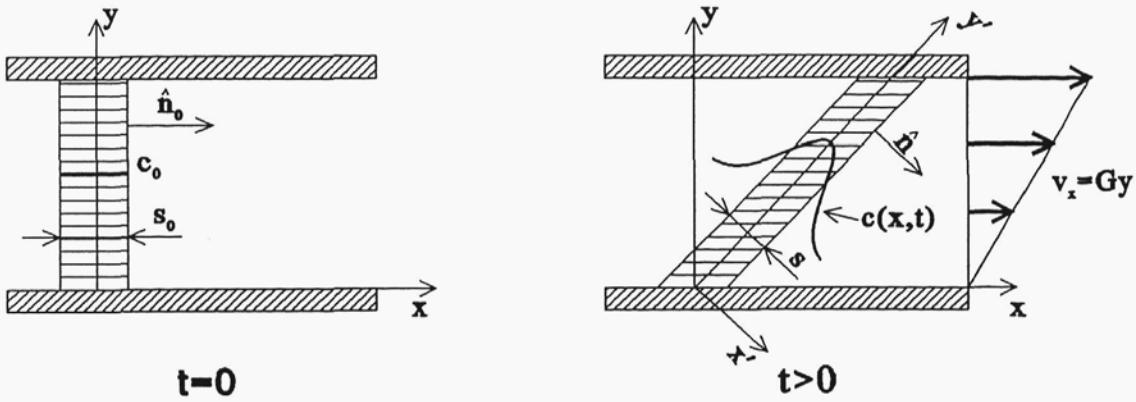

Figure 3.8. Mixing in a two-dimensional shear flow.

The slab of initial thickness s_0 contains inert tracer which diffuses outward the slab during the process of shearing. The slab initially perpendicular to the flow (versor $\hat{\mathbf{n}}$ parallel to $\vec{v}$) shrinks and rotates during the process. The shear flow is characterized by a single quantity, the shear rate - **G**:

$$v_x = G \cdot y \ , \quad v_y = 0 \ , \quad v_z = 0 \ . \tag{3.17}$$

In the local system of coordinates ($\mathbf{x}'$, $\mathbf{y}'$) rotating with the material surface the local rate of stretch is given by:

$$\alpha' = -\frac{1}{s} \cdot \frac{ds}{dt} = \frac{G^2 \cdot t}{1 + (G \cdot t)^2} \ , \tag{3.18}$$

so the slab shrinks due to:

$$s = s_0 / \sqrt{1 + (G \cdot t)^2} \ . \tag{3.19}$$

Equation (3.18) shows that at **t=0** the rate of deformation is equal to zero. The rate of stretch - α' gradually increases with time and reaches the maximum of α'_{max}=**G/2** at **t=1/G** when $\hat{\mathbf{n}}$ is declined 45° degrees from the initial orientation; 45° is the direction of the fastest stretching in the shear flow. The non-vanishing rotation moves the slab through the optimum orientation and the rate of the slab shrinking decreases. For long mixing time (**t≫1/G**) the rate of deformation decreases proportionally to **1/t** approaching finally zero, when **t** → ∞. Notice, that for **t** → ∞ similarly as at **t=0** the versor $\hat{\mathbf{n}}$ has a diagonal orientation with the respect to principal axes of deformation. Assuming the one-dimensional distribution of the tracer in the slab, mixing in the local frame of reference which rotates with the slab is described by:

$$\frac{\partial c}{\partial t} + \frac{x'}{s} \cdot \frac{ds}{dt} \cdot \frac{\partial c}{\partial x'} = D \cdot \frac{\partial^2 c}{\partial x'^2} \tag{3.20a}$$

with the boundary and initial conditions:

$$c(x' \to \pm\infty, t) = 0 \ , \tag{3.20b}$$

$$c(x',0) = \begin{cases} 0 & x' \le -s_0/2 \\ 1 & -s_0/2 < x' < s_0/2 \\ 0 & s_0/2 \le x' \end{cases} \ . \tag{3.20c}$$

The analytical solution of equations (3.20) is given by expression (3.9) in terms of dimensionless variables (3.7). The relation between the "warped time" and the physical time is given now by:

$$\tau = \frac{D}{s_0^2} \cdot \left(t + \frac{1}{3} \cdot G^2 \cdot t^3 \right) . \tag{3.21}$$

Thus, the real mixing time required to decrease twice the concentration of diffusive tracer at the center of the slab is equal to

$$t_{s1/2} = \frac{1}{G} \cdot \left[\left(\sqrt{\upsilon^2 + 1} + \upsilon \right)^{1/3} - \left(\sqrt{\upsilon^2 + 1} - \upsilon \right)^{1/3} \right] , \tag{3.22}$$

where

$$\upsilon = 1.5 \cdot \tau_{1/2} \cdot G \cdot s_0^2 / D \cong 0.412 \cdot G \cdot s_0^2 / D \ . \tag{3.23}$$

If the shear rate - **G** is equal to zero, then the mixing time - $\mathbf{t_{s1/2}}$ reaches the upper bound -

$t_{D1/2}$ given by equation (3.12), similarly as in the case of $t_{E1/2}$. When the shear rate increases $t_{S1/2}$ tends to zero. Comparison of $t_{E1/2}$ and $t_{S1/2}$ shows influence of the orientation on the mixing rate.

The rate of elongation - α and the shear rate - **G** are related through the rate of energy dissipation per unit volume, which in Newtonian liquids reads:

$$\epsilon = 2 \cdot \mu \cdot \left[\left(\frac{\partial v_x}{\partial x} \right)^2 + \left(\frac{\partial v_y}{\partial y} \right)^2 + \left(\frac{\partial v_z}{\partial z} \right)^2 \right] + \mu \left[\left(\frac{\partial v_x}{\partial y} + \frac{\partial v_y}{\partial x} \right)^2 + \left(\frac{\partial v_x}{\partial z} + \frac{\partial v_z}{\partial x} \right)^2 + \left(\frac{\partial v_y}{\partial z} + \frac{\partial v_z}{\partial y} \right)^2 \right] . \qquad \textbf{(3.24)}$$

Thus for the elongational flow defined by equation (2.12) one receives:

$$\epsilon = 2 \cdot \mu \cdot \left[\left(\frac{\partial v_x}{\partial x} \right)^2 + \left(\frac{\partial v_y}{\partial y} \right)^2 \right] = 4 \cdot \mu \cdot \alpha^2 , \qquad \textbf{(3.25)}$$

so

$$\alpha = \sqrt{\epsilon / \mu} / 2 . \qquad \textbf{(3.26)}$$

In the case of shear flow defined by equation (3.17) expression (3.24) yields:

$$\epsilon = \mu \cdot \left(\frac{\partial v_x}{\partial y} \right)^2 = \mu \cdot G^2 , \qquad \textbf{(3.27)}$$

so

$$G = \sqrt{\epsilon / \mu} . \qquad \textbf{(3.28)}$$

Thus comparing expressions (3.26) and (3.28) one receives:

$$G = 2 \cdot \alpha \qquad \textbf{(3.29)}$$

and

$$t_F = \frac{2}{G} . \qquad \textbf{(3.30)}$$

The mixing times $t_{E1/2}$ and $t_{S1/2}$ are compared in figure 3.9.

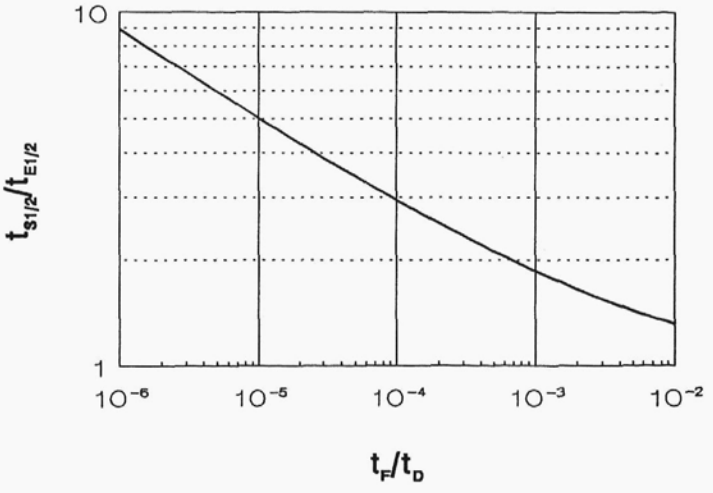

Figure 3.9. Comparison of $t_{E1/2}$ with $t_{S1/2}$.

The simple shear mixing time $t_{S1/2}$ is longer than the elongation mixing time $t_{E1/2}$. This effect results from continuous variation of slab orientation in the shear flow due to rotation. Both elongation rates are equal only at $t=1/(2\alpha)$; for $t<1/(2\alpha)$ and $t>1/(2\alpha)$ one has $\alpha' < \alpha$ (compare equations (3.18), (3.26) and (3.28)).

Mixing which proceeds by simultaneous deformation and diffusion has another interesting feature. It can be shown that when an inert tracer diffuses outside a liquid element which is elongated with a constant rate, the penetration distance of the tracer substance stabilizes after some time. To show this let us come back to the situation shown in figure 3.2, but now with the initial condition (3.6c) of the more general form:

$$c(x,0) = f(x) \ . \tag{3.31}$$

f(x) is an arbitrary function of **x** integrable in the interval $<-s_0/2, s_0/2>$ and $\mathbf{f(x)} \equiv \mathbf{0}$ behind this interval. In this case the concentration profile expressed in terms of dimensionless variables (3.7) is given by [65,p.53]:

$$C(\xi,\tau) = \frac{1}{2\cdot\sqrt{\pi\cdot\tau}} \cdot \int_{-1/2}^{-1/2} f(\eta\cdot s_0)\cdot\exp\left[-\frac{(\xi-\eta)^2}{4\cdot\tau}\right] d\eta \tag{3.32}$$

or, for α=**const**:

$$c(x,t) = \sqrt{\frac{\alpha}{2\cdot\pi\cdot D(e^{2\alpha t}-1)}} \cdot \int_{-s_0/2}^{s_0/2} f(u)\cdot\exp\left[-\frac{\alpha\cdot(x\cdot e^{\alpha t}-u)^2}{2\cdot D\cdot(e^{2\alpha t}-1)}\right] du \ . \tag{3.33}$$

Normalizing now the concentration profile (3.33) with the use of tracer concentration at **x**=0 and using the mean-value theorem (appendix A) one has:

$$c_\infty(x) = \lim_{t\to\infty} \frac{c(x,t)}{c(0,t)} = \exp\left(-\frac{\alpha\cdot x^2}{2\cdot D}\right) . \tag{3.34}$$

Figure 3.10 shows the time evolution of the normalized profile for the case when **f(x)** is given by (3.6c). As it can be seen the limiting universal profile is obtained for times comparable with $\mathbf{t_{E1/2}}$.

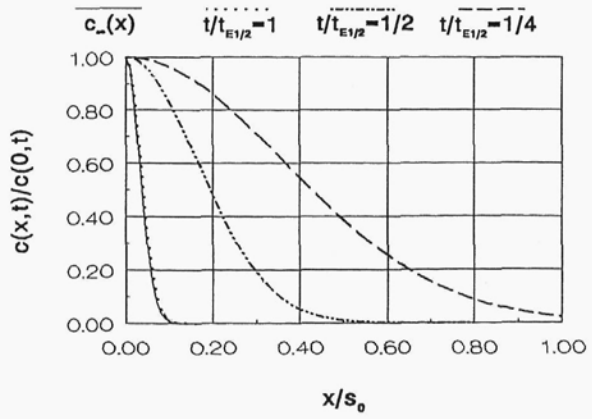

Figure 3.10a. $\mathbf{t_F/t_D=10^{-3}}$.

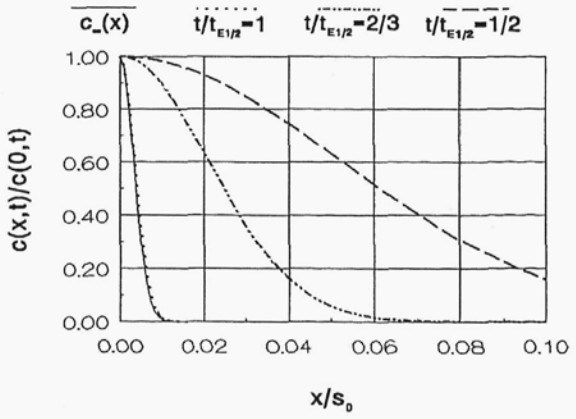

Figure 3.10b. $\mathbf{t_F/t_D=10^{-5}}$.

Stabilization of normalized concentration profiles

Defining now the limiting tracer penetration distance, l_∞ as the distance between the coordinate origin and the point where the concentration of the tracer equals 1% of the maximum one finds from (3.34):

$$l_\infty = \sqrt{\ln 10^4 \cdot D/\alpha} \cong 3 \cdot \sqrt{D/\alpha} \qquad (3.35)$$

It should be noticed that both: the limiting profile, $\mathbf{c}_\infty$, and the penetration distance, l_∞, do not depend on the initial distribution of the tracer, **f(x)**.

Very similar results can be obtained in axisymmetric system, when a tracer substance is allowed to diffuse outside the elongated filament. For the flow defined below:

$$v_r = -\alpha \cdot r/2 \ , \quad v_\theta = 0 \ , \quad v_z = \alpha \cdot z \ , \qquad (3.36)$$

one has elongation of the filament in the axial direction and contraction in the radial direction, as shown in figure 3.11.

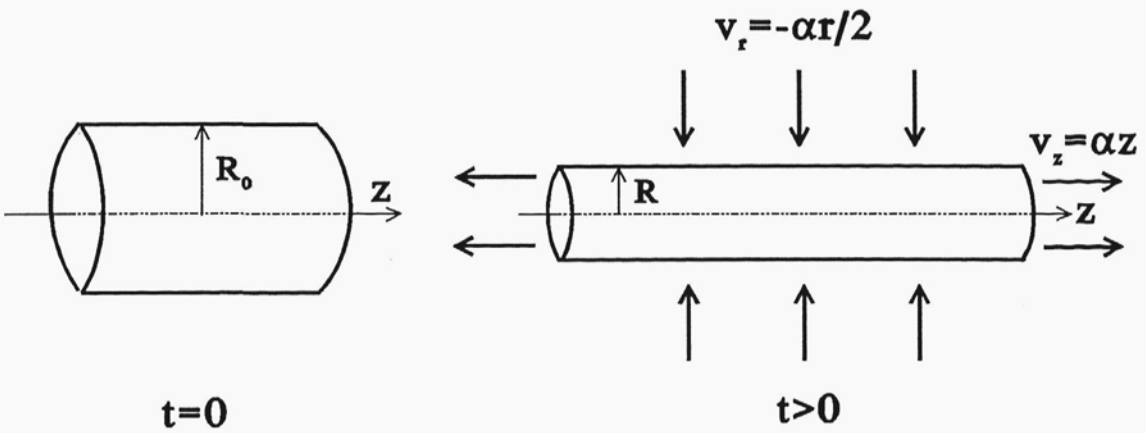

Figure 3.11. Elongation of a filament in an axisymmetric stagnation flow.

Neglecting changes in tangential and axial directions (one-dimensional concentration distribution) the tracer balance equation reads:

$$\frac{\partial c}{\partial t} + v_r \cdot \frac{\partial c}{\partial r} = \frac{D}{r} \cdot \frac{\partial}{\partial r}\left(r \cdot \frac{\partial c}{\partial r}\right) \qquad (3.37a)$$

with

$$\left.\frac{\partial c}{\partial r}\right|_{r=0} = 0 \ , \qquad (3.37b) \qquad\qquad c(r \to +\infty, t) = 0 \ , \qquad (3.37c)$$

$$c(r,0) = \begin{cases} f(r) & r \le R_0 \\ 0 & R_0 < r \end{cases} \ . \qquad (3.37d)$$

Solution of equations (3.37) (appendix B) reads:

$$c(r,t) = \frac{\alpha}{2 \cdot D \cdot (e^{\alpha t} - 1)} \cdot \int_0^{R_0} f(u) \cdot \exp\left(- \frac{\alpha}{4 \cdot D} \cdot \frac{r^2 \cdot e^{\alpha t} + u^2}{e^{\alpha t} - 1} \right) \cdot I_0 \left(\frac{\alpha}{2 \cdot D} \cdot \frac{u \cdot r \cdot e^{\alpha t/2}}{e^{\alpha t} - 1} \right) \cdot u \, du \ . \qquad (3.38)$$

So, the limiting normalized concentration profile becomes:

$$c_\infty(r) = \lim_{t \to \infty} \frac{c(r,t)}{c(0,t)} = \exp\left(- \frac{\alpha \cdot r^2}{4 \cdot D} \right) \qquad (3.39)$$

and the limiting penetration radius, l_∞ ($\mathbf{c_\infty(l_\infty)=0.01}$), is given by

$$l_\infty = \sqrt{\ln 10^8 \cdot D/\alpha} \cong 4.3 \cdot \sqrt{D/\alpha} \ . \qquad (3.40)$$

In all presented examples the molecular diffusion process was assumed to be one-dimensional. In reality molecular diffusion is a three-dimensional phenomenon. However, deformation affects the process in such a way that molecular diffusion in deformed fluid elements quickly becomes one-dimensional. To show this phenomenon let us consider an instantaneous reaction between **A** and **B**

$$A + B \overset{k \to \infty}{\rightarrow} P \qquad (3.41)$$

performed in a three-dimensional space in a two-dimensional stagnation flow.
Initially $\mathbf{N_B}$ moles of reactant **B**, is concentrated in the point **(x,y,z)=(0,0,0)**. The rest of the space is occupied by reactant **A** of initial concentration $\mathbf{c_{A0}}$. Both reactants have the same coefficients of molecular diffusion $\mathbf{D_A=D_B=D}$, so instead of $\mathbf{c_A}$ and $\mathbf{c_B}$ one can use a single composition variable [66]:

$$c = c_B - c_A \ , \qquad (3.42)$$

which reduces the problem to single equation:

$$\frac{\partial c}{\partial t} + \alpha \cdot x \cdot \frac{\partial c}{\partial x} - \alpha \cdot y \cdot \frac{\partial c}{\partial y} = D \cdot \left(\frac{\partial^2 c}{\partial x^2} + \frac{\partial^2 c}{\partial y^2} + \frac{\partial^2 c}{\partial z^2} \right) . \qquad (3.43)$$

Using dimensionless variables:

$$X = \frac{x}{L} \ , \quad Y = \frac{y}{L} \ , \quad Z = \frac{z}{L} \ , \quad T = \alpha \cdot t \ , \quad C = \frac{c}{c_{A0}} \ , \qquad (3.44)$$

where **L** is a characteristic length scale of the process

$$L = \sqrt{D/\alpha} \qquad (3.45)$$

one can transform equation (3.43) into:

$$\frac{\partial C}{\partial T} + X \cdot \frac{\partial C}{\partial X} - Y \cdot \frac{\partial C}{\partial Y} = \frac{\partial^2 C}{\partial X^2} + \frac{\partial^2 C}{\partial Y^2} + \frac{\partial^2 C}{\partial Z^2} \ . \qquad \textbf{(3.46a)}$$

Equation (3.46a) should be solved with the boundary and initial conditions:

$$C(X,Y,Z,0) = (\beta + 1) \cdot \delta(X,Y,Z) - 1 \ , \qquad \textbf{(3.46b)}$$

$$C(X \to \pm\infty, Y \to \pm\infty, Z \to \pm\infty, T) = -1 \ , \qquad \textbf{(3.46c)}$$

where δ**(X,Y,Z)** is delta function and constant β is defined as

$$\beta = N_B / \left(L^3 \cdot c_{A0} \right) \ . \qquad \textbf{(3.47)}$$

Following Townsend [67], the solution of equations (3.46) is given by:

$$C = \frac{1}{(2 \cdot \pi)^{3/2}} \cdot \frac{\beta}{a \cdot b \cdot c} \cdot \exp\left[-\frac{1}{2} \cdot \left(\frac{X^2}{a^2} + \frac{Y^2}{b^2} + \frac{Z^2}{c^2} \right) \right] - 1 \ , \qquad \textbf{(3.48)}$$

where

$$a^2 = e^{2 \cdot T} - 1 \ , \quad b^2 = 1 - e^{-2 \cdot T} \ , \quad c^2 = 2 \cdot T \ . \qquad \textbf{(3.49)}$$

Equation (3.48) allows to determine the position of reaction surface from condition **C=0** (at reaction surface $\mathbf{c_A = c_B = 0}$). Figure 3.12 shows time evolution of the intersection of the reaction surface at **Z=0**. For short times ($\mathbf{t \ll 1/\alpha}$), **B**-rich zone grows with similar rate in both directions due to molecular diffusion. For times approaching the characteristic deformation time - $\mathbf{1/\alpha}$ the shape of reaction surface stabilizes. For longer times, the reaction zone shrinks due to chemical reaction. Notice that for $\mathbf{T \gg 1}$ $\mathbf{b^2 \ll a^2}$ and $\mathbf{b^2 \ll c^2}$, so the gradient components **(∂C/∂Z)** and **(∂C/∂X)** are much smaller than **(∂C/∂Y)** and diffusion in direction of **Y** dominates in the process. Thus the initially isotropic process of molecular mass transfer becomes quickly one-dimensional and goes so fast in direction of **Y** that can compete with convective mixing.

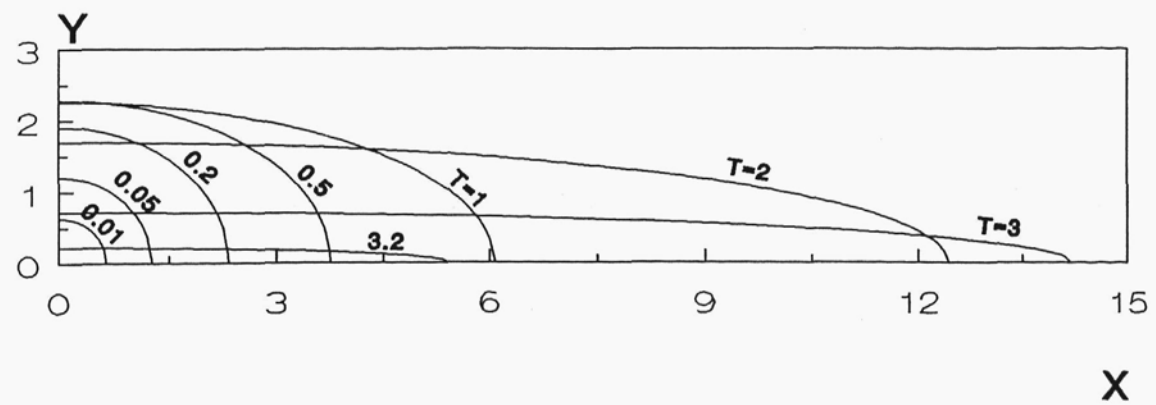

Figure 3.12a. Time evolution of the reaction surface; Z=0, β=1000.

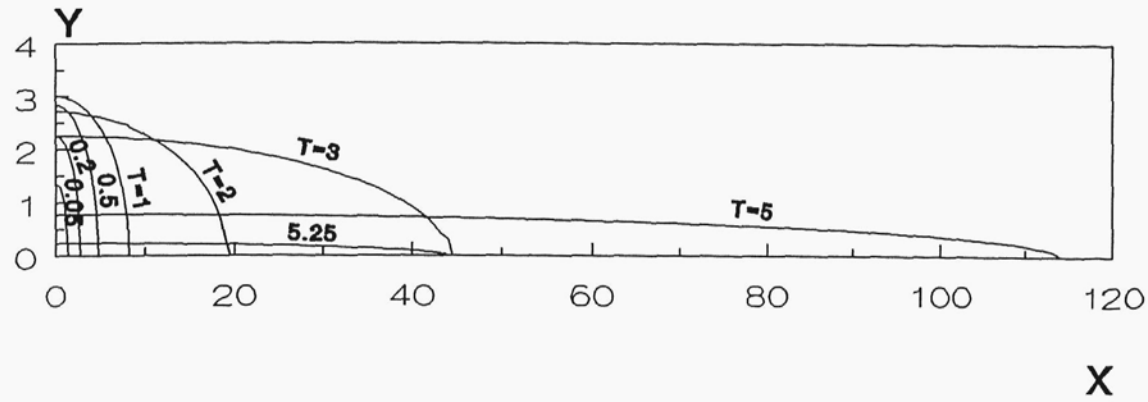

Figure 3.12b. Time evolution of the reaction surface; Z=0, β=10000.

Presented examples explain the role of deformation in mixing on the molecular scale: generation of an intermaterial area, decreasing of segregation scale, increasing of concentration gradients and the relation between stretching and orientation.

Growth of concentration gradients is observed in the direction of contraction, whereas their decline is observed in the direction of stretching. This observation is useful for modelling of micromixing, as it allows in many cases to consider mixing on the molecular scale as one-dimensional process.

It should also be pointed out that stretching of liquid elements tends to stabilize the penetration distance of the diffusive solutes. The time necessary to stabilize the profile is of the order of $t_{E1/2}$ and the shape of the limiting profile depends on the stretching geometry and the ratio of the constants for deformation and diffusion.

3.2. Effects of Physical Properties of Mixed Media on the Course of Mixing.

Laminar mixing can be strongly influenced by physical properties of mixed liquids. This influence takes different forms in single-phase and multi-phase systems. Mixing of multi-phase systems generally is not considered in this thesis; some information about two-phase liquid-liquid systems seems to be necessary for comparison.

There is a strong evidence in the literature [34,50,53,54] that mixing of immiscible or partially miscible liquids usually results in dispersion of the minor component into droplets (though there are examples that the minor component forms a continuous phase [68]). The primary reason for break-up of the minor component striations or filaments into drops is interfacial tension. Interfacial tension, σ, is responsible for discontinuity of the normal stress, $\overrightarrow{\sigma}$, at the liquid-liquid interface: